Calculation of the photoionization cross section of N_2 from first threshold to 500 Å

H. C. TUCKWELL†

Department of Mathematical Physics, University of Adelaide, South Australia

MS. received 3rd February 1969, in revised form 9th October 1969

Abstract. A method of determining photoionization cross sections for homonuclear diatomic molecules is outlined. For the initial electronic states self-consistent field–linear combination of atomic orbitals–molecular orbital wave functions constructed from Slater type atomic orbitals are used. A preliminary calculation is performed using two-centre Coulomb waves for the final electronic states. The quantum-defect approach to finding phase shifts is investigated but uncertainties in the interpretations of Rydberg series of molecular states makes if difficult to obtain reliable continuum functions. Results are given for photoionizing transitions in $N_2(X\,^1\Sigma_g^+)$ which give rise to the states $N_2{}^+(X\,^2\Sigma_g^+, A\,^2\Pi_u, B\,^2\Sigma_u^+)$. The vibrational states are accounted for with Franck–Condon factors.

1. Introduction

There have been many experimental advances in the study of photoionization of diatomic molecules over extensive frequency ranges in the last two decades. Whereas the theoretical work for atoms has made considerable progress (Marr 1967), calculations of the cross sections for molecules have been limited to a few, chiefly because of the lack of suitable wave functions for the bound and free electronic states. Calculations have appeared for $H_2{}^+$ (Bates *et al.* 1953) where the Schrödinger equation can be written down and solved accurately for the electronic motion. For many-electron systems it is necessary to find suitable approximate electronic eigenfunctions. This has been achieved for H_2 (Flannery and Öpik 1965), methane (Dalgarno 1952), and more recently for the π electrons of ethylene, butadiene, and benzene (Kaplan and Markin 1968 a, b). The results obtained by Flannery and Öpik for H_2 were encouraging in their agreement with the experimentally determined cross sections at and near threshold. This suggests that their model may provide a suitable basis for calculations on more complex systems if the continuum states can be suitably modified to allow for the greater departures from the potential of the two half elementary charges system in such cases. In many ways their model can be considered to bear the same relationship to the diatomic molecular problem as an ordinary Coulomb potential with $Z = 1$ does to the problem of finding continuum states for electrons moving in the field of an atomic ion. This is the chief line of thought in the calculations to be presented, though our approach cannot claim to be as rigorous as that in similar calculations for atoms because the necessary mathematical theories have not yet been fully developed. The final state chosen by Kaplan and Markin is only suitable for calculations at high energies. For studies of N_2 and O_2, however, the regions of greatest interest are, in view of the atmospheric and astrophysical applications, at and near the thresholds for ionization. Further, we do not restrict the kind of initial state and find cross sections for processes involving σ and π molecular orbitals (MO's) of g and u symmetry. At low energies of the ejected electron the vibrational contributions to the transition probabilities must be included to obtain the true variation of the cross sections with energy.

† Now at Committee on Mathematical Biology, University of Chicago, Chicago, Illinois, U.S.A.

2. General theory

The theory of atomic photoionization has been outlined by Burgess and Seaton (1960) and their approach can be used for diatomic molecular systems in the following way. If we adopt the notation of Herzberg (1967), the initial state wave function for the transition is designated $\Psi_i(\Lambda, S, M_S, v, J|\boldsymbol{r}, \boldsymbol{R})$, where $\boldsymbol{r}$ and $\boldsymbol{R}$ are the electronic and nuclear coordinates; Λ, S, M_S are the quantum numbers describing the electronic state; v and J are the vibrational and rotational quantum numbers. We let a final state of the system be $\Psi_f(\Lambda', S', M_S', v', J', e', k^2|\boldsymbol{r}, \boldsymbol{R})$ where e' denotes the quantum numbers of the continuum orbital and k^2 represents its energy. The photoionization cross section for the transition from Ψ_i to Ψ_f is then given by

$$\sigma(k^2) = \frac{4\pi\alpha a_0{}^2/3}{(2S+1)\epsilon_\Lambda} \sum{}' (I+k^2) \left| \int\int \Psi_i \boldsymbol{M} \Psi_f \, d\boldsymbol{r} \, d\boldsymbol{R} \right|^2 \tag{1}$$

where α is the fine structure constant, a_0 is the Bohr radius, I is the ionization potential in rydbergs and $\boldsymbol{M}$ is the dipole length operator for the collection of charges. The factor $(2S+1)\epsilon_\Lambda$ is the statistical weight of the initial electronic state, ϵ_Λ being the Neumann factor ($\epsilon_\Lambda = 1$ if $\Lambda = 0$, $\epsilon_\Lambda = 2$ otherwise). The summation is over degenerate initial and final states and k^2, the energy of the photoelectron in rydbergs, is determined by the conservation of energy condition.

The dipole selection rules are $\Delta\Lambda = 0, \pm 1$, $\Delta S = \Delta M_S = 0$, and for the electron making the transition $\Delta m = 0, \pm 1$ where m is the magnitude of the electron's angular momentum along the internuclear axis in units of $\hbar$. There are also restrictions on the symmetry of the final states that can combine with a given initial state. These are as usual that g and u states only combine and that $\Sigma^{+,-}$ and $\Sigma^{+,-}$ states can only combine. For equation (1) to be valid we require the normalization conditions

$$\int\int \bar{\Psi}_i \Psi_i \, d\boldsymbol{r} \, d\boldsymbol{R} = 1 \tag{2}$$

$$\int\int \bar{\Psi}_f(k^2) \Psi_f(k'^2) \, d\boldsymbol{r} \, d\boldsymbol{R} = \delta(k^2 - k'^2) \tag{3}$$

to be satisfied.

We can write $\boldsymbol{M}$ as the sum of an electronic component $\boldsymbol{M}_e$ and a nuclear component $\boldsymbol{M}_n$. Further, in the Born–Oppenheimer approximation we can write a molecular wave function as the product of an electronic part $\psi_{el}(\Lambda, S, M_S|\boldsymbol{r}, \boldsymbol{R})$, and a part which describes the rotational and vibrational states $\psi_{vib}(v, J|R)\psi_{rot}(J|\hat{\boldsymbol{R}})$. If we define

$$\boldsymbol{M}_{fi} = \int\int \bar{\Psi}_i (\boldsymbol{M}_e + \boldsymbol{M}_n) \Psi_f \, d\boldsymbol{r} \, d\boldsymbol{R} \tag{4}$$

and assume that $\boldsymbol{M}_n$ does not depend on the electronic coordinates, then by virtue of the orthogonality of the initial and final electronic states the term involving $\boldsymbol{M}_n$ vanishes. This means that the sum in (1) becomes simply

$$\sum{}' (I+k^2) \left| \int\int \bar{\Psi}_i \left(\sum_{i=1}^{N} \boldsymbol{r}_i \right) \Psi_f \, d\boldsymbol{r} \, d\boldsymbol{R} \right|^2 \tag{5}$$

where N is the number of electrons, and again k^2 is, for a given pair of initial and final states, determined by the relation

$$k^2 = h\nu - I + E(v_i, J_i) - E(v_f, J_f) \tag{6}$$

where $h\nu$ is the incident photon energy, I is the difference in energies between the zero vibrational and rotational levels of the initial and final systems, and $E(v_i, J_i)$ and $E(v_f, J_f)$ are measured relative to those levels respectively. The expression (1) does not contain explicit reference to the statistical weights of the initial vibrational and rotational levels. These can be accounted for by the appropriate Boltzmann factors. However, at standard temperatures only the zeroth vibrational level is appreciably occupied by the systems of interest here and, furthermore, the inclusion of rotational eigenstates is not expected to have a significant effect on the final results, so the Boltzmann factors are not included.

3. Cross sections for fixed nuclei

Following the approach of Bates *et al.* (1953) and Flannery and Öpik (1965) it is useful as a first step in the calculations to consider the ionization process as a purely electronic transition and evaluate the matrix elements for fixed internuclear separation. In this case we ignore the vibrational and rotational contributions and determine the cross section as

$$\sigma_0(k^2) = \frac{4\pi\alpha a_0{}^2/3}{(2S+1)\epsilon_\Lambda} \times (I+k^2) \sum{}' \left| \int \bar{\Psi}_{\mathrm{i}}(\Lambda, S, M_S|\boldsymbol{r}) \left(\sum_{i=1}^{N} \boldsymbol{r}_{\mathrm{i}} \right) \Psi_{\mathrm{f}}(\Lambda', S', M_S', e'; k^2|\boldsymbol{r}) \, \mathrm{d}\boldsymbol{r} \right|^2. \quad (7)$$

3.1. *Electronic bound states*

The most convenient method of describing the electronic states of molecules is that of molecular orbitals. The one-electron wave functions are considered as the product of a spatial part (MO) and a spin function to give a molecular spin orbital (MSO). A given electronic configuration (a consignment of MSO's) can then be described by a Slater determinant, suitably normalized. Roothaan (1951) developed the theory of two approaches to the problem of determining the best MO's. The better but more difficult method results in the Hartree–Fock MO's while that which is more amenable to computational work finds the best LCAO–MO's. In the LCAO–MO approach an orthonormal set of atomic orbitals is used to construct an MO wave function.

Many calculations of SCF–LCAO–MO's for various molecules have appeared. Those of special interest here are those of Scherr (1955) for N_2 and of Sahni and Lorenzo (1965) who treated several electronic states of N_2, $N_2{}^+$, O_2 and $O_2{}^+$. The set of atomic orbitals used are the real Slater type with a specially constructed 2s function. To evaluate the cross sections we find it convenient to work in prolate spheroidal coordinates so we now find expressions for the relevant one-electron MO's in terms of these.

Letting R be the internuclear separation, we find that an LCAO $\pi_{\mathrm{u}}\,2\mathrm{p}$ wave function can be written $\psi(\pi_{\mathrm{u}}\,2\mathrm{p}|\lambda, \mu) \exp(\pm \mathrm{i}\phi)$ with

$$\psi(\pi_{\mathrm{u}} 2\mathrm{p}|\lambda, \mu) = C(\beta, R)(\lambda^2-1)^{1/2}(1-\mu^2)^{1/2} \exp(-\beta\lambda) \cosh(\beta\mu) \quad (8)$$

where $C(\beta, R)$ is a normalization constant; $\beta = \zeta_2 R/2$, ζ_2 being the orbital exponent for the Slater 2p AO. The fact that we are no longer using a real MO means only a change in $C(\beta, R)$. The properties of the wave functions under the operation of inversion can be found by making the transformations $\lambda \to \lambda$, $\mu \to -\mu$, $\phi \to \phi+\pi$, and clearly the above expression for the $\pi_{\mathrm{u}}\,2\mathrm{p}$ MO possesses u symmetry. Similarly if we write a σ_{g} MO wave function

$$\psi(\sigma_{\mathrm{g}}|\boldsymbol{r}) = a_1\psi_1(\sigma_{\mathrm{g}}1\mathrm{s}|\boldsymbol{r}) + a_2\psi_2(\sigma_{\mathrm{g}}2\mathrm{s}|\boldsymbol{r}) + a_3\psi_3(\sigma_{\mathrm{g}}2\mathrm{p}|\boldsymbol{r}) \quad (9)$$

where the wave functions on the right-hand side represent primitive molecular orbitals (Scherr 1955), we find, on using

$$r_1 \cos\theta_1 = Z_1 = Z + \tfrac{1}{2}R = \tfrac{1}{2}(\lambda\mu+1)R \quad (10)$$

$$r_2 \cos\theta_2 = Z_2 = \tfrac{1}{2}R - Z = \tfrac{1}{2}(1-\lambda\mu)R \quad (11)$$

that in prolate spheroidal coordinates we have

$$\psi(\sigma_{\mathrm{g}}|\lambda, \mu) = c_1 \exp(-\gamma\lambda)\cosh(\gamma\mu) + R\{(c_2\lambda + c_3)\cosh(\beta\mu) - (c_2 + c_3\lambda)\mu\sinh(\beta\mu)\}\exp(-\beta\lambda) \tag{12}$$

$$c_1 = \left(\frac{2\zeta_1^3}{\pi}\right)^{1/2}\left\{a_1 - \frac{a_2 S_i}{(1-S_i^2)^{1/2}}\right\} \tag{13}$$

$$c_2 = a_2\left\{\frac{\zeta_2^5}{6\pi(1-S_i^2)}\right\}^{1/2}, \qquad c_3 = a_3\left(\frac{\zeta_2^5}{2\pi}\right)^{1/2} \tag{14}$$

$$S_i = (1\mathrm{s}|2\mathrm{s}) = \frac{24\zeta_1\zeta_2^2(\zeta_1\zeta_2/3)^{1/2}}{(\zeta_1+\zeta_2)^4} \tag{15}$$

ζ_1 being the orbital exponent for the Slater 1s AO, and we have put $\gamma = \frac{1}{2}\zeta_1 R$. In (10) and (11) the indices 1 and 2 refer to the two nuclei. Further, if we write a σ_{u} LCAO–MO wave function

$$\psi(\sigma_{\mathrm{u}}|\boldsymbol{r}) = a_1\psi_1(\sigma_{\mathrm{u}}1\mathrm{s}|\boldsymbol{r}) + a_2\psi_2(\sigma_{\mathrm{u}}2\mathrm{s}|\boldsymbol{r}) + a_3\psi_3(\sigma_{\mathrm{u}}2\mathrm{p}|\boldsymbol{r}) \tag{16}$$

then we have

$$\psi(\sigma_{\mathrm{u}}|\lambda, \mu) = -c_1\exp(-\gamma\lambda)\sinh(\gamma\mu) + R\{(c_3\lambda + c_2)\mu\cosh(\beta\mu) - (c_3 + c_2\lambda)\sinh(\beta\mu)\}\exp(-\beta\lambda). \tag{17}$$

3.2. *Electronic continuum states*

For calculations of atomic photoionization cross sections several forms of continuum function for the ejected electron have been used. Amongst these are plane waves, ordinary Coulomb waves for $Z = +1$ or some effective nuclear charge, modified Coulomb waves with phase shifts calculated from bound-state energy data by the extrapolated quantum-defect method (QDM) and also the Hartree or Hartree–Fock solutions. If an approximate solution to the Schrödinger equation is being sought then the choice of the continuum function is determined by the energy range and the details of the system in question. Plane waves are only accurate at high energies and spherical Coulomb waves can only be used at low energies if the phase shifts of the final states are small. In the case of electrons ejected from atoms containing several electrons the phase shifts can be estimated reliably by the quantum-defect method (Seaton 1958), and thus an accurate continuum function can be found in the asymptotic region, at large distances from the core.

The simplest type of wave function appropriate for the positive energy states of an electron in the field of a diatomic ion is a two-centre Coulomb wave. If the charge on each centre is $+\frac{1}{2}e$ and we write $\psi(\lambda, \mu, \phi|k^2)$ as the product of three parts, then these satisfy

$$\frac{\mathrm{d}}{\mathrm{d}\lambda}\left\{(\lambda^2-1)\frac{\mathrm{d}\Lambda}{\mathrm{d}\lambda}\right\} + \left\{h^2\lambda^2 - A_l^m(h) + R\lambda - \frac{m^2}{\lambda^2-1}\right\}\Lambda = 0 \tag{18}$$

$$\frac{\mathrm{d}}{\mathrm{d}\mu}\left\{(1-\mu^2)\frac{\mathrm{d}M}{\mathrm{d}\mu}\right\} + \left\{A_l^m(h) - h^2\mu^2 - \frac{m^2}{1-\mu^2}\right\}M = 0 \tag{19}$$

$$\frac{\mathrm{d}^2\Phi}{\mathrm{d}\phi^2} = -m^2\Phi \tag{20}$$

where $h = \frac{1}{2}kR$, m^2 and $A_l^m(h)$ being separation constants. The solutions of (20) can be written $\exp(\pm \mathrm{i}m\phi)$, m integer (twofold degeneracy if $m \neq 0$) and the solutions to (19) have been given by Stratton *et al.* (1956) and Morse and Feshbach (1953) as

$$M_l^m(h, \mu) = \sum_{n=0}^{\infty}{}' d_n(h|m, l)P^m_{n+m}(\mu); \qquad l = m, m+2, \ldots \tag{21a}$$

which is an even function of μ, the odd solution being

$$M_l^m(h, \mu) = \sum_{n=1}^{\infty}{}' d_n(h|m, l)P^m_{m+n}(\mu); \qquad l = m+1, m+3, \ldots \tag{21b}$$

Σ' here means summation over alternate values of n and the coefficients $d_n(h|m, l)$ of the associated Legendre functions have been tabulated at certain values of h by Stratton *et al.* (1956) whose tables can also be used to find the $A_l^m(h)$.

A study of equation (18) shows that its two independent solutions behave as $(\lambda-1)^{m/2}$ and $(\lambda-1)^{-m/2}$ near $\lambda = 1$. If we write $\chi_l^m(h, \lambda) = (\lambda^2-1)^{1/2}\Lambda_l^m(h, \lambda)$ then

$$\frac{d^2\chi}{d\lambda^2}+\left\{\frac{R\lambda+h^2\lambda^2-A_l^m(h)}{\lambda^2-1}+\frac{1-m^2}{(\lambda^2-1)^2}\right\}\chi = 0. \tag{22}$$

If we denote the solutions of this equation which are regular and irregular near $\lambda = 1$ by G_l^m and H_l^m respectively then we seek a suitable linear combination L_l^m to represent the solution to the present problem at large λ.

We now turn our attention to the asymptotic region. If the term $R\lambda$ is missing in equation (22) then the solutions G and H for the free-particle problem have asymptotic forms

$$G \underset{\lambda\to\infty}{\simeq} \cos(h\lambda+\tfrac{1}{2}(l+1)\pi) \tag{23}$$

$$H \underset{\lambda\to\infty}{\simeq} \sin(h\lambda+\tfrac{1}{2}(l+1)\pi) \tag{24}$$

(Morse and Feshbach 1953, p. 1505 *et seq.*). We expect the corresponding solutions to (22) to have these forms with a two-centre Coulomb phase shift. The logarithmic term can be found by Stokes' method (Buckingham 1962) and is $k^{-1}\ln 2h\lambda$, but sufficient study of the solutions to (22) has not been made to enable us to write an explicit form for the constant term corresponding to $\arg\Gamma(l+1+i\gamma)$ for spherical Coulomb waves. As argued by Flannery and Öpik (1965), we assume that the solutions for an electron in the field of a diatomic ion have asymptotic forms

$$L_l^m(h, \lambda) \underset{\lambda\to\infty}{\simeq} \cos\{h\lambda+k^{-1}\ln 2h\lambda+\tfrac{1}{2}(l+1)\pi+\delta_l^m(h)+\pi\mu'(h)\} \tag{25}$$

where $\mu'(h)$ is the extrapolated quantum defect. A proof that the quantum defect can be employed in this manner has not yet appeared so this approach can only be considered a useful approximation at present. However, the quantum-defect method has been employed and its validity established to some extent in applications to electron–molecular-ion scattering (Weinberg *et al.* 1968).

To calculate the quantum defects we note that for very high members of a Rydberg series of two-centre Coulomb bound states ($Z = \frac{1}{2}e$) the energy levels can be closely approximated by $-1/n^2$ rydbergs where n is the principal quantum number in the united atom designation. Thus for the high members of a Rydberg series of diatomic molecular states we can obtain the quantum defects from

$$E_{n,l,\lambda'} = \frac{1}{(n-\mu_{n,l,\lambda'})^2} \tag{26}$$

(cf. Weinberg *et al.* 1968) where $E_{n,l,\lambda'}$ is the energy in rydbergs to remove an electron whose state is $(nl\lambda')$ in the united atom designation (λ' is the component of angular momentum along the internuclear axis in units of $\hbar$).

The quantum-defect method enables us to obtain the final-state waves in the asymptotic region. To evaluate the matrix elements it is necessary to obtain an approximate solution at small distances from the centre of the ion (Burgess and Seaton 1960). Thus we write

$$L_l^m(h,\lambda) = C_l^m(h)\{G_l^m \cos(\pi\mu') - f_l^m(h,\lambda)H_l^m \sin(\pi\mu')\} \tag{27}$$

where G_l^m and H_l^m are solutions to (22) and $f_l^m(h, \lambda)$ is a cut-off factor designed to diminish the contributions from the irregular solution near $\lambda = 1$. A suitable form was found to be

$$f_l^m(h,\lambda) = [1-\exp\{-\tau_l^m(h)(\lambda-1)\}]^{2l+m+1} \tag{28}$$

which ensured that the solutions did not diverge in this region. Furthermore, the values of the τ_l^m were obtained by the criterion that $f_l^m(h, \lambda)$ should not approach unity until the irregular solution H_l^m has become oscillatory, the first node of this function being taken as the critical point.

3.3. *Evaluation of the electronic matrix elements for closed shells*

A molecule in which all MO's are filled must be in a $^1\Sigma$ state so that $(2S+1)\epsilon_\Lambda = 1$ and the allowed final states are $^1\Sigma$ and $^1\Pi$. In a process in which an electron from a given MO is ejected we ignore all other electrons except those which have the same spatial wave function. For a σ MO there are two eigenstates and we choose as initial state the antisymmetrized two-electron wave function

$$\Psi_i(X_1, X_2) = 2^{-1/2}\{\psi_1(1)\psi_2(2) - \psi_1(2)\psi_2(1)\} \tag{29}$$

and for the final state

$$\Psi_f(X_1, X_2) = 2^{-1}\{\psi_1(1)\psi_k(2) - \psi_1(2)\psi_k(1) + \psi_k(1)\psi_2(2) - \psi_k(2)\psi_2(1)\} \tag{30}$$

where ψ_1 and ψ_2 are the bound-state MSO's and ψ_k describes the continuum state. If we assume that the wave functions for the passive electrons are almost unchanged in the process (which should be valid for the systems being considered here) then the dipole length matrix element between Ψ_i and Ψ_f is

$$\boldsymbol{M}_{fi} = \frac{1}{\sqrt{2}}\left\{\int \bar{\psi}_1(\boldsymbol{r})\boldsymbol{r}\psi_k(\boldsymbol{r})\,\mathrm{d}\boldsymbol{r} + \int \bar{\psi}_2(\boldsymbol{r})\boldsymbol{r}\psi_k(\boldsymbol{r})\,\mathrm{d}\boldsymbol{r}\right\}. \tag{31}$$

Since ψ_1 and ψ_2 are identical spatial wave functions we have

$$|\boldsymbol{M}_{fi}|^2 = 2\left|\int \bar{\psi}(\sigma|\lambda,\mu)\boldsymbol{r}\psi_k(\lambda,\mu,\phi)\,\mathrm{d}\boldsymbol{r}\right|^2. \tag{32}$$

To obtain explicit forms for the various components of $\boldsymbol{M}_{fi}$ we note that

$$\begin{aligned} x &= \left(\frac{R}{4}\right)(\lambda^2-1)^{1/2}(1-\mu^2)^{1/2}\{\exp(\mathrm{i}\phi)+\exp(-\mathrm{i}\phi)\} \\ y &= \left(\frac{R}{4\mathrm{i}}\right)(\lambda^2-1)^{1/2}(1-\mu^2)^{1/2}\{\exp(\mathrm{i}\phi)-\exp(-\mathrm{i}\phi)\} \\ z &= \left(\frac{R}{2}\right)\lambda\mu. \end{aligned} \tag{33}$$

For the x and y components we obtain contributions from final states with $m = \pm 1$.

For the z component, $m = 0$ only and we have for the sum over final states

$$\sum_{\mathrm{f}} |\boldsymbol{M}_{\mathrm{fi}}|^2 = 2\sum_{l} \{|\mathscr{M}_z^{\,l}|^2 + 4|\mathscr{M}_x^{\,l}|^2\} \tag{34}$$

where l is odd for σ_{g} initial states and l is even for σ_{u} initial states. Explicitly we have

$$\mathscr{M}_z^{\,l} = \frac{R^4\pi}{8}\int_1^\infty\int_{-1}^1 \bar{\psi}(\sigma|\lambda,\mu)(\lambda\mu)(\lambda^2-\mu^2)\Lambda_l^0(h|\lambda)M_l^0(h|\mu)\,\mathrm{d}\mu\,\mathrm{d}\lambda \tag{35}$$

$$\mathscr{M}_x^{\,l} = \frac{R^4\pi}{16}\int_1^\infty\int_{-1}^1 \bar{\psi}(\sigma|\lambda,\mu)(\lambda^2-1)^{1/2}(1-\mu^2)^{1/2}(\lambda^2-\mu^2) \times\Lambda_l^1(h|\lambda)M_l^1(h|\mu)\,\mathrm{d}\mu\,\mathrm{d}\lambda. \tag{36}$$

The expressions which result when $\psi(\sigma_{\mathrm{g}}|\lambda,\mu)$ and $\psi(\sigma_{\mathrm{u}}|\lambda,\mu)$, given by (12) and (17) respectively, are substituted in (35) and (36) are too lengthy to be displayed here.

For filled π MO's we must use four-electron initial states

$$\Psi_{\mathrm{i}}(\boldsymbol{X}_1,\boldsymbol{X}_2,\boldsymbol{X}_3,\boldsymbol{X}_4) = (4!)^{-1/2}\sum_p(-)^p\psi_1(\boldsymbol{X}_1)\psi_2(\boldsymbol{X}_2)\psi_3(\boldsymbol{X}_3)\psi_4(\boldsymbol{X}_4) \tag{37}$$

where $\Sigma_p(-)^p\ldots$ is the Slater determinant. The final states must then be described by a linear combination of determinantal functions

$$\Psi_{\mathrm{f}}(\boldsymbol{X}_1,\boldsymbol{X}_2,\boldsymbol{X}_3,\boldsymbol{X}_4) = 2^{-1}(4!)^{-1/2}\{\sum_p(-)^p\psi_k\psi_2\psi_3\psi_4 + \sum_p(-)^p\psi_1\psi_k\psi_3\psi_4 + \sum_p(-)^p\psi_1\psi_2\psi_k\psi_4 + \sum_p(-)^p\psi_1\psi_2\psi_3\psi_k\}. \tag{38}$$

It is more convenient to ignore configuration interaction so that

$$\sum{}' |\boldsymbol{M}_{\mathrm{fi}}|^2 = \sum_{j=1}^{4}\sum_{\Lambda'}\left|\int\bar{\psi}_j(\boldsymbol{r})\boldsymbol{r}\psi(k,\Lambda'|\boldsymbol{r})\,\mathrm{d}\boldsymbol{r}\right|^2 \tag{39}$$

where ψ indicates a spatial part of an electron wave function. Noting that

$$\psi_1(\boldsymbol{r}) = \psi_2(\boldsymbol{r}) = \psi(\pi|\lambda,\mu)\exp(\mathrm{i}\phi)$$

and that

$$\psi_3(\boldsymbol{r}) = \psi_4(\boldsymbol{r}) = \psi(\pi|\lambda,\mu)\exp(-\mathrm{i}\phi)$$

we find

$$\sum{}' |\boldsymbol{M}_{\mathrm{fi}}|^2 = 2\sum_{\Lambda'}\left\{\left|\int\bar{\Psi}_1(\boldsymbol{r})\boldsymbol{r}\psi(k,\Lambda'|\boldsymbol{r})\mathrm{d}\boldsymbol{r}\right|^2 + \left|\int\bar{\Psi}_3(\boldsymbol{r})\boldsymbol{r}\psi(k,\Lambda'|\boldsymbol{r})\,\mathrm{d}\boldsymbol{r}\right|^2\right\}. \tag{40}$$

The x component of $\boldsymbol{M}_{\mathrm{fi}}$ has contributions from final states with $m = 0, \pm 2$, the y component has contributions from $m = 0, \pm 2$ (these being equal to those for the x component with the same value of m) and the z component has contributions from $m = \pm 1$ only. Summing over degenerate final states then gives

$$\sum{}' |\boldsymbol{M}_{\mathrm{fi}}|^2 = 4\sum_{l}\{|\mathscr{M}_z^{\,l,\pi}|^2 + 2|\mathscr{M}_x^{\,l,\sigma}|^2 + 2|\mathscr{M}_x^{\,l,\delta}|^2\} \tag{41}$$

where σ, π and δ refer to final states with $m = 0, \pm 1$ and ± 2 respectively, and again summation is over odd l for π_{g} initial states and over even l for π_{u} initial states. For the quantities in (41) we have

$$\mathcal{M}_x^{l,\sigma} = \frac{R^4\pi}{16}\int_1^\infty\int_{-1}^1 \bar{\psi}(\pi|\lambda,\mu)(\lambda^2-1)^{1/2}(1-\mu^2)^{1/2}(\lambda^2-\mu^2)\Lambda_l^0(h|\lambda)M_l^0(h|\mu)\,\mathrm{d}\mu\,\mathrm{d}\lambda \tag{42}$$

$$\mathcal{M}_z^{l,\pi} = \frac{R^4\pi}{8}\int_1^\infty\int_{-1}^1 \bar{\psi}(\pi|\lambda,\mu)(\lambda\mu)(\lambda^2-\mu^2)\Lambda_l^1(h|\lambda)M_l^1(h|\mu)\,\mathrm{d}\mu\,\mathrm{d}\lambda \tag{43}$$

$$\mathcal{M}_x^{l,\delta} = \frac{R^4\pi}{16}\int_1^\infty\int_{-1}^1 \bar{\psi}(\pi|\lambda,\mu)(\lambda^2-1)^{1/2}(1-\mu^2)^{1/2}(\lambda^2-\mu^2)\Lambda_l^2(h|\lambda)M_l^2(h|\mu)\,\mathrm{d}\mu\,\mathrm{d}\lambda. \tag{44}$$

The evaluation of such expressions as (42) follows from (8) and (21) or (22). For an initial π_u 2p MO we have

$$\mathcal{M}_x^{l,\sigma} = \frac{CR^4\pi}{8}\int_1^\infty (\lambda^2-1)\exp(-\beta\lambda)\Lambda_l^0(h|\lambda) \times\left(\sum_{n=0}^{\infty}{}' \mathrm{d}_n(h|0,l)[\lambda^2\{A_n(\beta)-B_n(\beta)\}+C_n(\beta)-B_n(\beta)]\right)\mathrm{d}\lambda \tag{45}$$

where

$$A_n, B_n, C_n = \int_{-1}^1 \mathrm{P}_n(\mu)\cosh(\beta\mu)(1,\mu^2,\mu^4)\,\mathrm{d}\mu. \tag{46}$$

To evaluate angular integrals such as these we define

$$\mathrm{J}_n(\beta) = \int_0^1 \mu^n\cosh(\beta\mu)\,\mathrm{d}\mu \tag{47}$$

whereupon, for example,

$$A_n(\beta) = \sum_{r=0}^{n/2}\frac{(-)^r(2n-r)!\mathrm{J}_{n-2r}(\beta)}{2^{n-1}r!(n-r)!(n-2r)!} \tag{48}$$

and the evaluation of the J_n is facilitated by the use of the recurrence relation

$$\mathrm{J}_n = \beta^{-(n+1)}\{\beta^n\sinh\beta - n\beta^{n-1}\cosh\beta + n(n-1)\beta^{n-1}\mathrm{J}_{n-2}\}. \tag{49}$$

Similar expressions may be developed for all the other matrix elements given above. Further, the asymptotic amplitudes of the normalized continuum radial functions have been given by Bates *et al.* (1953) and these can be obtained directly from the appropriate functions $\Phi(\phi)$ and $M(\mu)$ given by $\exp(\pm im\phi)$ and (21*a*) or (21*b*) respectively.

4. Rydberg series of N_2

An important part of the calculations is the determination of the quantum defects for the continuum states by extrapolation from those for Rydberg series of bound states. Data on such series converging to the states X $^2\Sigma_g^+$, A $^2\Pi_u$ and B $^2\Sigma_u^+$ of N_2^+ has been given by Ogawa and Tanaka (1962) who extended the Worley–Jenkins series, Worley's third series and the Hopfield series as well as discovering new Rydberg series converging to the A $^2\Pi_u$ and B $^2\Sigma_u^+$ states of the ion. A more recent investigation (Carroll and Yoshino 1967) has found another series which converges to the state N_2^+ (X $^2\Sigma_g^+$). The interpretation of these Rydberg series is uncertain in most cases and before the quantum defects can be extrapolated to the continuum the electronic configurations of the Rydberg states must be ascertained. Because there are so many final states in the case of photoionization of diatomic molecules involving a given initial MO wave function, and a correspondingly large number of possible Rydberg states, it is not a straightforward matter to interpret the series. We make the following assumption in determining the appropriate configuration of the Rydberg series of states. That, if the cross sections in absorption for high members in a Rydberg series in which the excited electron is in the $(nl\lambda')$ state are large, then the cross sections for transitions in which the ejected electron is in the positive energy state $(k^2l\lambda')$ will be large provided k^2 is small. That the absorption should be continuous at the series limit was predicted by Sugiura, though the experimental work on absorption cross sections for atoms has indicated that this is often only approximately true (Marr 1967, p. 104). Possibly the best confirmation yet observed for the continuity can be found in the results of Burgess and Seaton (1960) for bound–bound and bound–free transitions in lithium.

4.1. *Rydberg series converging to $N_2^+(X\,^2\Sigma_g^+)$*

Our calculations of the cross sections for the case $\mu' = 0$ (corresponding to Flannery and Öpik's final-state model), which are discussed in § 5.1, show that the greatest contribution near threshold, for the process in which a $\sigma_g 2p$ electron is ejected, comes from $p\sigma_u$ final states. We should, according to the assumption above, interpret the Worley–Jenkins series, extended by Ogawa and Tanaka (1962), as the progression $(\sigma_g 2p)(np\sigma_u)\,^1\Sigma_u^+ \leftarrow (\sigma_g 2p)^2\,^1\Sigma_g^+$, where $n = 4, 5, 6 \ldots$ (the $3p\sigma_u$ shell is already filled). Carroll and Yoshino (1967) have suggested, however, that only the first member of the series reported by Ogawa and Tanaka belongs to the $np\sigma_u\,^1\Sigma_u^+$ progression and that the higher members belong to the $np\pi_u\,^1\Pi_u$ progression. It turns out that the different interpretations give practically the same result for the extrapolated quantum defects. In our calculations we used the data of Carroll and Yoshino but, since the $p\pi_u$ final states only contribute to a minor extent, we did not employ QDM phase shifts for their evaluation.

4.2. *Rydberg series converging to N_2^+ $(A\,^2\Pi_u)$*

Two Rydberg series have been observed which converge to this state, the stronger being known as Worley's third series (Ogawa and Tanaka 1962). Calculations employing zero phase shifts show that the main contributions near threshold are from the $d\pi_g$ and $d\delta_g$ continua. If we employ our previous assumption (§ 4) we should associate Worley's third series with the progression

$$(\pi_u 2p)^3(nd\pi_g)\,^1\Sigma_u^+ \leftarrow (\pi_u 2p)^4\,X\,^1\Sigma_g^+$$

and the weak series with

$$(\pi_u 2p)^3(nd\delta g)\,^1\Pi_u \leftarrow (\pi_u 2p)^4\,X\,^1\Sigma_g^+.$$

Ogawa and Tanaka are fairly sure, however, that the third series consists of $ns\sigma_g$ final states and this claim agrees with Mulliken's previous interpretation. This gives large quantum defects ($\simeq 2$) which seem plausible for s electrons. Furthermore, Ogawa and Tanaka claim that their weak series has its first member missing so that a reasonable interpretation is the $nd\pi_g$ sequence, $n = 3, 4, 5 \ldots$, giving quantum defects near unity which again seems plausible (p electrons in separated atoms designation). Furthermore, the state $(\pi_u 2p)^3(\sigma_g 2p)^2(\pi_g 2p)b'\,^1\Sigma_u^+$ is close to the expected first member of the weak series. We therefore used the second interpretation of the Rydberg series in computing the results given in § 5.4. The $s\sigma_g$ continuum is very weak, however, so phase shifts were not employed for their evaluation. Furthermore, no data are available for estimating the quantum defects of the $d\delta_g$ continuum for which the phase shifts should be small, so large errors should not be incurred.

4.3. *Rydberg series converging to N_2^+ $(B\,^2\Sigma_u^+)$*

The electronic configurations of the upper states of the two Rydberg sereis which have been found to approach this state of N_2^+ have not been ascertained. Our calculations with $\mu' = 0$ showed that transitions to the $d\sigma_g$ and $d\pi_g$ continua are by far the strongest, with the former dominating slightly. The assumption used leads to the identification of Ogawa and Tanaka's strong and weak series as the progressions

$$(\sigma_u 2p)(nd\sigma_g)\,{}^1\Sigma_u^+ \leftarrow (\sigma_u 2p)^2\ \mathrm{X}\,{}^1\Sigma_g^+$$

and

$$(\sigma_u 2p)(nd\pi_g)\,{}^1\Pi_u \leftarrow (\sigma_u 2p)^2\ \mathrm{X}\,{}^1\Sigma_g^+$$

respectively, with $n = 3, 4, 5 \ldots$ in both cases. However, the ionization energy of the first member of the weak series is far too small (less than 2 ev) to interpret as due to excitation to a $3d\pi_g$ state. The conclusion that the strong series corresponds to $nd\sigma_g$ ($n = 3, 4, 5 \ldots$) and that the weak series corresponds to $nd\pi_g$ ($n = 3, 4, 5 \ldots$) with the first member missing is consistent with the assumption and the approximate energy-level diagram for N_2 (Herzberg 1967, p. 329). This is also consistent with Mulliken's alternative interpretation of the Hopfield series.

5. Results for N_2

5.1. *Numerical procedures*

Most of the techniques required for performing these calculations have been given by Bates *et al.* (1953) and can be employed in the present case if allowance is made for the change in magnitude of the charge on each centre from $+e$ to $+\frac{1}{2}e$.

The ranges of the radial variable λ at which the functions G_l^m, H_l^m, L_l^m, and the bound-state functions were determined are: 1·0(0·05)3·0; 3·0(0·1)7·0; 7·0(0·2)10·8. The evaluation of G_l^m is straightforward if a power series is used near $\lambda = 1$ and a recurrence relation employed to extend the calculations to larger λ. The computation of H_l^m cannot be achieved in the same manner. However, in the asymptotic region the values of H_l^m can be obtained directly from the corresponding G_l^m by utilizing the amplitude and phase functions for these solutions (Buckingham 1962, Wheeler 1937). If we let $G_l^m = C(\lambda)\cos X(\lambda)$ and $H_l^m = C(\lambda)\sin X(\lambda)$ in the asymptotic region then we can find the value of $C(\lambda)$ from a series, the first terms being

$$C_l^m(h,\lambda) = d_l^m(h)\left[1 - \frac{1}{2hk}\lambda^{-1} + (A_l^m + \tfrac{5}{2}k^{-2} - h^2)\left(\frac{1}{2hk}\right)^2\lambda^{-2} + \ldots\right] \tag{50}$$

where $d_l^m(h)$ is the asymptotic amplitude of the unnormalized solutions (cf. Bates *et al.* 1953). The phase relation of G_l^m and H_l^m is then utilized to obtain values of H_l^m at two neighbouring values of λ from

$$H_l^m(\lambda) = \pm\{C(\lambda)^2 - G_l^m(\lambda)^2\}^{1/2} \tag{51}$$

the positive or negative root being taken if the derivative of G_l^m is negative or positive respectively. These values of H_l^m can then be employed to start an inward integration by the recurrence relation method. This approach is most reliable if (51) is employed near a node of G_l^m. Unfortunately the zero energy functions cannot be found by this method but an approximate determination of $C(\lambda)$ can be made from the computed G_l^m and the error should not be large. Once the functions G_l^m and H_l^m are tabulated it is a simple matter to compute the required solution (27).

5.2. *Partial cross sections for various ion states using ordinary two-centre Coulomb waves*

The three ionizing transitions considered here are

$$N_2(\mathrm{X}\,{}^1\Sigma_g^+) + h\nu \to N_2^+(\mathrm{X}\,{}^2\Sigma_g^+,\ \mathrm{A}\,{}^2\Pi_u,\ \mathrm{B}\,{}^2\Sigma_u^+) + e \tag{52}$$

corresponding to removal of $\sigma_g 2p$, $\pi_u 2p$ and $\sigma_u 2s$ electrons with thresholds at photon wavelengths of 796 Å (15·6 ev), 743 Å (16·7 ev) and 661 Å (18·8 ev) respectively (Cook and Metzger 1964). In figure 1 are shown the cross sections for these processess evaluated at the following values of the energy variable h: 0(0·1)1·0; 1·0(0·2)2·2; 3(1)5. We now discuss briefly the results for each orbital type.

5.2.1. $N_2(X\,^1\Sigma_g^+)+h\nu \rightarrow N_2^+(X\,^2\Sigma_g^+)+e$. The cross section is high at threshold due mainly to transitions to the pσ_u continuum. As h increases the contributions from pσ_u and pπ_u final states drop rapidly while the cross sections for the fσ_u and fπ_u continua increase and finally dominate, giving rise to the peak near 250 Å. This

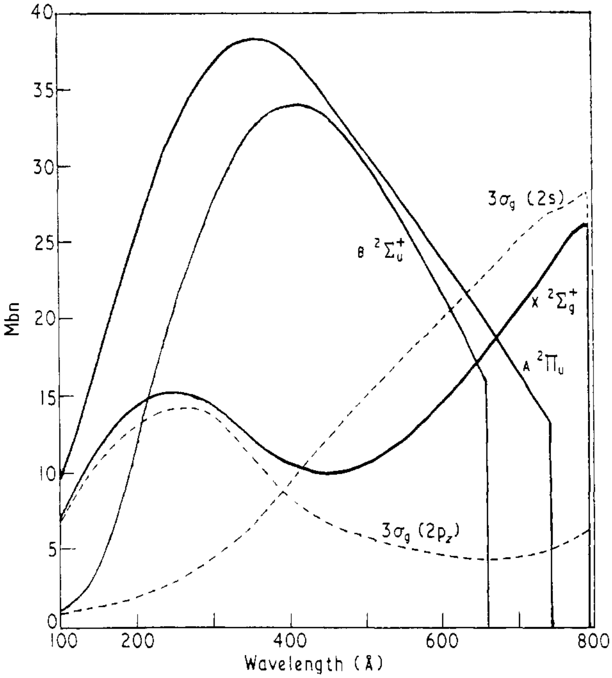

Figure 1. Calculated photoionization cross sections for processes which leave N_2^+ in various states using ordinary two-centre Coulomb waves for the ejected electron are shown by the full curves. The broken curves show the cross sections for $3\sigma_g$ molecular orbitals synthesized from either 2s atomic orbitals or $2p_z$ atomic orbitals only.

phenomenon is interesting in view of its prediction by Cohen and Fano (1966) in relation to the shoulders observed in the experimental absorption cross sections of Samson and Cairns (1965). A previous calculation (Bates and Öpik 1968) which employed similar final-state waves failed to produce an appreciable contribution from the higher angular momentum states at higher energies, so that the nature of the initial state must be the critical factor. We pursued this matter further and calculated the cross sections for σ_g MO's consisting of 2s atomic orbitals only and $2p_z$ atomic orbitals only, these results also being shown in figure 1. The cross section for a non-hybrid σ_g 2s initial state is high at threshold and diminishes steadily at higher energies, displaying in fact very similar behaviour to Bates and Öpik's (1968) results for a model complex molecule. In contrast the cross section for a $\sigma_g\,2p_z$ non-hybrid orbital is low at and near threshold and, after a slight decrease, increases to give a peak at about 250 Å.

5.2.2. $N_2(X\,^1\Sigma_g^+)+h\nu \rightarrow N_2^+(A\,^2\Pi_u)+e$. The major contributions are for the dπ_g and dδ_g continua at and near threshold and these continua remain dominant throughout almost the whole energy range. Both show an increase until $h \simeq 1$ (421 Å) followed by a fairly rapid decrease, so that the cross section exhibits the same behaviour. Of the higher angular momentum states only gπ_g gives a significant contribution at higher energies, but in the main range of energies it never dominates the process. Consequently no high-energy peak arises in the cross section.

5.2.3. $N_2(X\,^1\Sigma_g^+)+h\nu \to N_2^+(B\,^2\Sigma_u^+)+e$. The two continua which dominate this process are $d\sigma_g$ and $d\pi_g$, both of which rise in transition strength from threshold. The $s\sigma_g$ continuum also rises but the cross section for this is negligible in comparison. Again no secondary peak arises due to higher angular momentum states, there being a single peak after threshold followed by a rapid decrease at higher energies.

5.3. *Inclusion of the vibrational states*

Considering the matrix elements in (5) in the Born–Oppenheimer approximation and employing simple rigid rotator eigenfunctions $Y_J^{M_J}$ for the rotational states, we have on integrating over the nuclear angular coordinates

$$|M_{fi}|^2 = \left|\int\int \bar{\psi}_{el}^{\,init}(\boldsymbol{r}, R)\bar{\psi}_{vib}^{\,init}(v, J|R)\{\Sigma \boldsymbol{r}\}\psi_{el}^{\,final}(\boldsymbol{r}, R) \times \psi_{vib}^{\,final}(v', J|R)\, d\boldsymbol{r}\, R^2\, dR\right|^2. \tag{53}$$

On assuming that the electronic wave functions do not depend on the nuclear radial variable R this becomes, in the usual notation,

$$\left|\int \bar{P}(v, J|R)P(v', J|R)\, dR \int \bar{\psi}_{el}^{\,init}(\boldsymbol{r})\{\Sigma \boldsymbol{r}\}\psi_{el}^{\,final}(\boldsymbol{r})\, d\boldsymbol{r}\right|^2 = q(v', v)\left|\int \bar{\psi}_{el}^{\,init}(\boldsymbol{r})\{\Sigma \boldsymbol{r}\}\psi_{el}^{\,final}(\boldsymbol{r})\, d\boldsymbol{r}\right|^2 \tag{54}$$

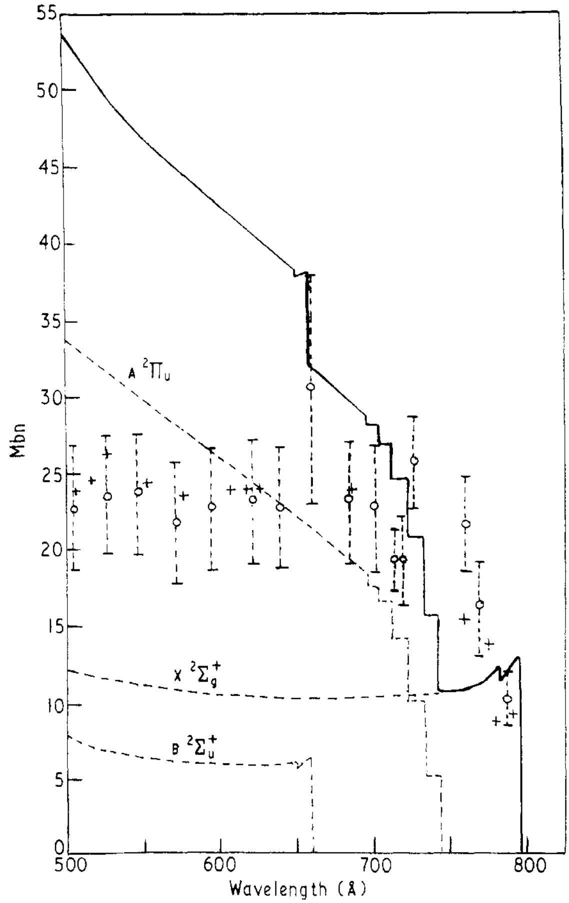

Figure 2. Calculated and experimental photoionization cross sections for N_2: ○ experimental, Wainfain *et al.* 1955; + experimental, Samson and Cairns 1964; broken curve, calculated partial cross sections for various ion states using QDM final-state waves; full curve, calculated total cross section.

where $q(v', v)$ is the Franck–Condon factor (Bates 1952). Calculations of the Franck–Condon factors for the ionizing transitions considered here have been performed by Nicholls (1961). The validity of reducing (53) to (54) will be enlarged upon in a later paper.

5.4. *Total cross section from* 796 Å *to* 500 Å

In figure 2 are shown the computed results for the three ionizing transitions mentioned above. In obtaining these results we have employed the QDM final-state waves for the ejected electrons (energy range to $h \simeq 1$) and Franck–Condon factors for the vibrational contributions. Also shown in figure 2 are the experimental results for the total photoionization cross sections of Wainfain *et al.* (1955) and Samson and Cairns (1964). For the sake of clarity in the figure we have restricted the number of experimental results, though there have been other investigations (Cook and Metzger 1964), including a determination of partial cross sections by photoelectron spectroscopy (Blake and Carver 1967). The calculated and experimental cross sections agree well from 796 Å to 661 Å. At higher energies there is considerable discrepancy, probably due to unreliable phase shifts in the continuum wave functions.

Acknowledgments

It is a pleasure to thank Professor C. A. Hurst for his constant encouragement throughout this work and to various members of the Adelaide University Physics Department, in particular Mr. J. Bahr, for many stimulating discussions.

References

Bates, D. R., 1952, *Mon. Not. R. Astr. Soc.*, **112**, 614–36.
Bates, D. R., and Öpik, U., 1968, *J. Phys.* B: *Atom. Molec. Phys.*, **1**, 543–7.
Bates, D. R., Öpik, U., and Poots, G., 1953, *Proc. Phys. Soc.* A, **66**, 1113–23.
Blake, A. J., and Carver, J. H., 1967, *J. Chem. Phys.*, **47**, 1038–44.
Buckingham, R. A., 1962, *Numerical Methods* (London: Issac Pitman).
Burgess, A., and Seaton, M. J., 1960, *Mon. Not. R. Astr. Soc.*, **120**, 121–51.
Carroll, P. K., and Yoshino, K., 1967, *J. Chem. Phys.*, **47**, 3073–4.
Cohen, H. D., and Fano, U., 1966, *Phys. Rev.*, **150**, 30–3.
Cook, G. R., and Metzger, P. H., 1964, *J. Chem. Phys.*, **41**, 321–36.
Dalgarno, A., 1952, *Proc. Phys. Soc.* A, **65**, 663–7.
Flannery, M. R., and Öpik, U., 1965, *Proc. Phys. Soc.*, **86**, 491–500.
Herzberg, G., 1967, *Spectra of Diatomic Molecules* (New York: Van Nostrand).
Kaplan, I. G., and Markin, A. P., 1968 a, *Opt. Spectrosc.*, **24**, 475–7.
—— 1968 b, *Opt. Spectrosc.*, **25**, 275–8.
Marr, G. V., 1967, *Photoionization Processes in Gases* (New York, London: Academic Press).
Morse, P. M., and Feshbach, H., 1953, *Methods of Theoretical Physics* (New York: McGraw-Hill).
Nicholls, R. W., 1961, *J. Res. Natn. Bur. Stand.* A, **65**, 451–60.
Ogawa, M., and Tanaka, Y., 1962, *Can. J. Phys.*, **40**, 1593–607.
Roothaan, C. C. J., 1951, *Rev. Mod. Phys.*, **23**, 69–89.
Sahni, R. C., and Lorenzo, E. J. De., 1965, *J. Chem. Phys.*, **42**, 3612–20.
Samson, J. A. R., and Cairns, R. B., 1964, *J. Geophys. Res.*, **69**, 4583–90.
—— 1965, *J. Opt. Soc. Am.*, **55**, 1035.
Scherr, C., 1955, *J. Chem. Phys.*, **23**, 569–78.
Seaton, M. J., 1958, *Mon. Not. R. Astr. Soc.*, **118**, 504–18.
Stratton, J. A., Morse, P. M., Chu, L. J., Little, J. D. C., and Corbato, F. J., 1956, *Spheroidal Wave Functions* (New York: John Wiley).
Wainfain, N., Walker, W. C., and Weissler, G. L., 1955, *Phys. Rev.*, **99**, 542–9.
Weinberg, M., Berry, R. S., and Tully, J. C., 1968, *J. Chem. Phys.*, **49**, 122–6.
Wheeler, J. A., 1937, *Phys. Rev.*, **52**, 1123–7.